CONTRASTING SHOCK MICROSTRUCTURE DEVELOPMENT IN ZIRCON FROM POROUS AND CRYSTALLINE TARGET LITHOLOGIES. Timmons M. Erickson[1,2] and David A. Kring[1,2], [1]Center for Lunar Science and Exploration, Lunar and Planetary Institute, USRA, 3600 Bay Area Blvd., Houston TX 77058 USA (Erickson@lpi.usra.edu), [2]NASA Solar System Exploration Research Virtual Institute.

Introduction: The utility of the mineral zircon, $ZrSiO_4$, as a shock-metamorphic geobarometer and geochronometer, has been steadily growing within the planetary science community. Zircon is an accessory phase found in many terrestrial rock types (e.g., [1]), lunar samples (e.g., [2]), lunar meteorites (e.g., [3]), martian meteorites (e.g., [4]) and various other achondrites (e.g., [5]). Because zircon is refractory and has a high closure temperature for Pb diffusion [6], it has been used to determine the ages of some of the oldest material on Earth [7] and elsewhere in the Solar System [5]. Furthermore, major (O) and trace-element (REE, Ti, Hf) abundances and isotope compositions of zircon help characterize the petrogenetic environments and sources from which they crystallized.

During shock deformation, resulting from hypervelocity impact, zircon behaves in unique, crystallographically-controlled ways. This includes dislocation creep and the formation of planar and subplanar low-angle grain boundaries, the formation of mechanical {112} twins [8, 9], transformation to the high pressure polymorph reidite [10, 11], the development of polycrystalline microtextures [12], and dissociation to the oxide constituents SiO_2 and ZrO_2 [13]. Shock microstructures can also variably affect the U-Th-Pb isotope systematics of zircon [14, 15] and, in some instances, be used to constrain the impact age.

While numerous studies have characterized shock deformation in zircon recovered from a variety of terrestrial impact craters (e.g., [14, 15, 16]) and Apollo samples [8], empirical studies of zircon deformation in different types of target rocks as a function of bulk shock pressures and temperatures recorded by the major phases (i.e., quartz and feldspar) are lacking. Here we address that issue with a systematic study of historic sample suites from the Ries impact structure, Germany, and Meteor Crater, USA. Specifically, we characterize and quantify deformation in zircon across a range of shock classes previously defined using other petrologic criteria. Because porous sedimentary and crystalline targets respond differently to shock, these two sample sets offer a unique opportunity to further constrain the behavior of zircon during shock across a range of geologic environments. This study will also help elucidate the bulk rheologic control of the target rock on the response of zircon to shock.

Geologic Background: The Ries Crater, also known as the Nördlinger Ries, is a ~25 km diameter,

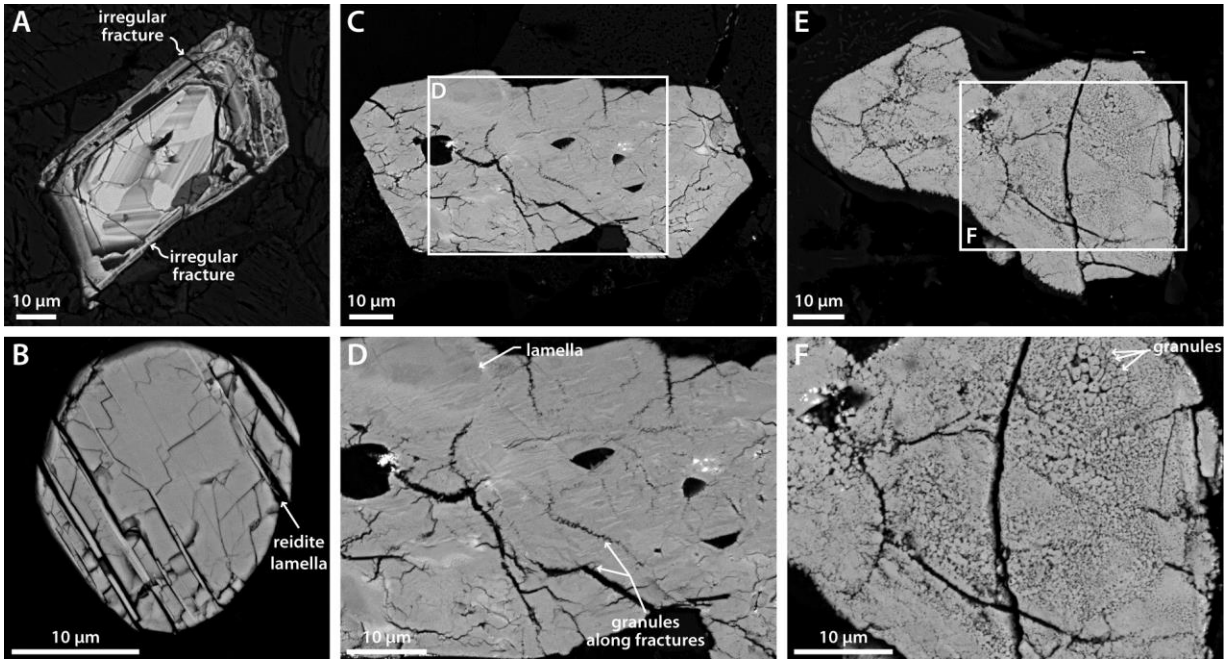

Figure 1. Backscattered electron images of progressive shock development in zircon from crystalline target rocks of the Ries Crater. (A) Unshocked zircon from shock stage 1 granite. (B) Shocked zircon with probable reidite lamellae (e.g., [11]) from a shock stage 2 biotite gneiss. (C-D) Zircon with discontinuous lamellae and granules from a shock stage III biotite-hornblende gneiss. (E-F) Polycrystalline zircon aggregate from an impact melt of granitic compositon.

14.8 Ma [17], complex crater located in southern Germany. It was produced from a two-layered target, composed of a thin ~700 m-thick cover of Mesozoic sediments and an underlying basement of gneisses and granites (e.g., [18]). Since recognition of the impact origin of the Ries crater [19], it has become the type locality for characterizing shock deformation of crystalline target rocks [20]. At shock stage 1 quartz and feldspar develop planar deformation features; at shock stage 2 diaplectic glasses form; at shock stage 3 localized melting occurs; and at shock stage 4 the whole rock undergoes melting [20]. Shocked zircon grains have been described at Ries with an array of deformation features [11, 13, 21]. To quantify the progressive development of shock deformation in zircon, this study utilizes the sample set of [20] to characterize zircon from granitic, gneissic, and amphibolitic target rocks across increasing shock classes.

Meteor Crater, also known as the Barringer Meteorite Crater, is a 1.2 km diameter, ca. 50 ka simple crater located on the Colorado Plateau of Arizona, USA [22]. The impactor punctured the porous sedimentary succession of Coconino Sandstone, Toroweap (sandstone) Formation, Kaibab (sandy dolomite) Formation, and Moenkopi (siltstone) Formation. Shock effects in quartz at Meteor Crater differ from those of the Ries in ways that have been attributed to the effect of porosity on the response to shock [23]. First, porosity is reduced and irregular fractures develop in quartz; secondly, planar fractures and minor shock lamellae develop; subsequently diaplectic SiO_2 glass forms along with minor coesite and stishovite symplectites; finally quartz completely melts and flow features form, known as lechatelierite. To constrain the progressive development of shock features in zircon from porous targets, a suite of Coconino Sandstone samples spanning the range of shock types is investigated.

Methods: Thin sections have been prepared from Ries Crater crystalline target rocks and Meteor Crater Coconino Sandstone target rocks that are representative of all shock classes. Petrographic observations of bulk shock conditions have been made in quartz and plagioclase where present. To characterize the range of shock features in zircon from within each sample, backscattered electron imaging and electron backscatter diffraction analyses are being undertaken.

Results: Shock development in zircon from the crystalline target rocks of the Ries crater systematically progress from brittlely deformed zircon with irregular fractures at shock stage 1 (Fig. 1a), to grains with planar microstructures including reidite lamellae (Fig. 1b), and possible {100} deformation bands and {112} shock twins at shock stage 2. Above shock stage 3 zircon display planar microstructures, recrystallized domains and minor granular texture (Fig. 1c-d), while zircon xenocrysts in impact melts are polycrystalline aggregates (Fig. 1e-f).

Zircon derived from the Coconino Sandstone show minimal shock effects until complete pore collapse occurs (at or above shock stage 1b of [23]). Zircon in shocked Coconino with diaplectic SiO_2 and coesite symplectites (shock stage 3-4 of [23]) are often brecciated and fractured, but grains containing microtwins and probable reidite are also preserved. Zircon grains from lechatelierite are polycrystalline, and other workers have found misorientation evidence for the former presence of shock twins and the conversion to reidite in these grains [12].

Summary: This work will help quantify the deformation mechanisms active in zircon under varying shock conditions. The rheological controls of different rock types and the affects of porosity on the development of shock features in zircon will also be constrained. Furthermore, subsequent *in situ* laser ablation mass spectrometry analyses of the U – Th – Pb systematics will identify the conditions appropriate for age resetting in zircon and will, therefore, help the interpretation of zircon age data from ancient craters and from *ex situ* zircon grains such as those in the lunar regolith.

References: [1] Hoskin P. W. O. & Schaltegger U. (2003) *Rev. in Min. and Geochem., 53,* 27–62. [2] Nemchin A. A. et al. (2009) *Nat. Geo. ,2,* 133–136. [3] Demidova S. I. et al. (2014) *Petrology*, 22, 1–16. [4] Humayun M. et al. (2013) *Nature, 503,* 513–516. [5] Ireland T. R. & Wlotzka F. (1992) *EPSL, 109,* 1–10. [6] Cherniak D. J. & Watson E. B. (2003) *Rev. in Min. and Geochem., 53,* 113–143. [7] Wilde S. A. et al. (2001) *Nature, 409,* 175–178. [8] Timms N. E. et al. (2012) *MAPS, 47,* 120–141. [9] Erickson T. M. et al. (2013) *Am. Min., 98,* 53–65. [10] Glass B. P. & Liu S. (2001) *Geology, 29,* 371 – 373. [11] Erickson T. M. et al. (2017) *Con. Min. Pet., 172*. [12] Cavosie A. J. et al. (2016) *Geology, 44,* 703–706. [13] Timms N. E. et al. (2017) *EPSL, 477,* 52–58. [14] Moser D. E. et al. (2011) *Can. J. Earth Sci., 48,* 117–139. [15] Schmieder M. et al. (2015) *GCA, 161,* 71 – 100. [16] Singleton A. C. et al. (2015) *GSA Special Publication 518,* 135–148. [17] Schmieder M. et al., (2018) *GCA, 220,* 146–157. [18] Stöffler D. (1977) Geol. Bavarica, 75, 443–458. [19] Shoemaker E. M. & Chao E. C. T. (1961) *JGR, 10,* 3371–3378. [20] Stöffler D. (1971) JGR, 76, 5541–5551. [21] Gucsik A. et al. (2004) *Cratering in Marine Environments and on Ice*, 281–322. [22] Kring D. A. (2017) *Guidebook to the Geology of Barringer Meteorite Crater, Arizona,* 272 p. [23] Kieffer S. W. 1971, *JGR, 76,* 5449–5473.